Sun Hazards and Solar Observing with the SMA
SMA Technical Memo #144
Scott Paine
April 9, 2001

Abstract

The sun can pose a significant hazard to a large reflector antenna. In a Cassegrain antenna with a long effective focal length, such as the SMA antennas, the greatest hazard does not occur when the sun is at boresight, since the image of the sun at the Cassegrain focus is fairly large. Rather, it occurs for a range of off-boresight positions where the compact, distorted image of the sun, formed by the primary reflector, lies near parts of the antenna or other nearby structures. This memo presents a quantitative analysis of the sun hazards associated with the SMA antennas. It is found that, provided the aluminum guards for the quadrupod are correctly assembled, a software sun-avoidance zone should be unnecessary. For solar observing, the main consideration is to avoid receiver saturation, which can be accomplished with a simple attenuator.

1. Introduction

Large reflector antennas are capable of collecting significant solar power and concentrating it in a small area. The consequent hazard to the antenna itself and to nearby objects can be serious. Sun-related accidents have occurred, for example, during assembly of the 15-metre SEST antenna on La Silla in Chile, and on two occasions during tests of the SMA antennas at Haystack observatory.

Various measures can be taken to avoid the problem. The reflector surface can be painted or grooved to reduce specular reflection of sunlight, but care must be taken not to introduce significant loss at signal frequencies. The antenna pointing software can maintain a sun-avoidance zone, but this is only effective when the antenna is under active control. Moreover, a sun-avoidance zone obviously precludes observations of the sun itself, and nearby objects.

The SMA antennas have been designed to point at or near the sun without sustaining damage. In principle, this makes a software sun avoidance zone unnecessary. This memo establishes a quantitative basis for this claim. Before going on, however, it should be emphasized that although the antennas themselves are well protected from the sun, personnel working around the antennas need to avoid exposing themselves, or flammable materials such as Eccosorb, to concentrated sunlight.

2. Reflectance of the SMA primary and secondary mirrors

Reflection of sunlight from the SMA primary is highly nonspecular due to the periodic grooves and random scratches produced during machining of the panel surface. These scatter incident sunlight into a broad arc perpendicular to the grooves. Because the grooves are circumferential, the scattered sunlight is further diluted azimuthally, except for an overlap region corresponding to the angular diameter of the sun, $\alpha_{sun} = 0.53^\circ$. Thus, for the purpose of estimating the concentration of sunlight by the antenna, the effective specular power reflectance of the primary, R_{eff}, may be taken as the fraction of collimated incident light which is reflected within a cone of angular diameter α_{sun} about the specular direction. Measurements of R_{eff} at 670 nm wavelength were made on a sample SMA panel in the receiver lab, in a plane of incidence perpendicular to the grooves, for various angles of incidence θ. The reflectance varies from $R_{eff} \approx 0.010$ near $\theta = 0^\circ$, to $R_{eff} \approx 0.021$ at $\theta = 45^\circ$. When the antenna is pointed at the sun, the range of incidence angles at the surface of the primary ranges from $\theta = 0^\circ$ near the vertex, to $\theta = 31^\circ$ (where $R_{eff} \approx 0.013$) near the rim. Nevertheless, in the remainder of this memo $R_{eff} = 0.02$ will be used as a conservative estimate.

The optical reflectance of the SMA secondary mirror, which is a diamond-turned aluminum surface protected by an SiO overcoat, is approximately $R_s = 0.9$.

3. Sun at boresight

With the sun at boresight, it is simple to estimate the intensities of the images of the sun formed at the primary and secondary foci of the antenna. At the primary focus, the diameter of the sun's image is

$$d_p = f_p \cdot \alpha_{sun}, \tag{1}$$

where $f_p = 2520$ mm is the focal length of the primary, giving $d_p = 23$ mm. The intensity at the image formed by the primary is

$$I_p = R_{eff} \cdot I_0 \cdot \left(\frac{D_p}{d_p} \right)^2, \tag{2}$$

where $D_p = 6$ m is the diameter of the primary and $I_0 = 1.4$ kW·m^{-2} is the solar constant. Taking $R_{eff} = 0.02$ gives $I_p = 1900$ kW·m^{-2}. Because the prime focus is blocked by the secondary when the sun is at boresight, this rather high intensity is never actually realized. When the sun is far enough off the boresight axis that its image is no longer blocked, distortion of the image reduces the peak intensity. This off-axis case is considered below.

At the Cassegrain focus, the effective focal length of the antenna is

$$f_c = F_c \cdot D_p, \tag{3}$$

where $F_c = 14$ is the focal ratio at the Cassegrain focus, giving $f_c = 84$ m. The diameter of the image of the sun at the Cassegrain focus is

$$d_c = f_c \cdot \alpha_{sun}, \tag{4}$$

or $d_c = 0.77$ m. Note that this is actually larger than the diameter of the secondary mirror, $D_s = 350$ mm. The intensity of the sun's image at the Cassegrain focus, neglecting truncation at the primary vertex aperture, elevation mirror M3, and elevation axis window, is

$$I_c = R_s \cdot R_{eff} \cdot I_0 \cdot \left(\frac{D_p}{d_c} \right)^2 \qquad (5)$$

or 1.5 kW·m^{-2}, approximately equal to I_0. Thus there is no solar hazard to equipment inside the receiver cabin. However, there is a potential eye hazard, which will be greatest at the cal load position between mirrors M4 and M5. The eye hazard is eliminated when the Gore-tex membrane, at the elevation axis window between M3 and M4, is in place.

It is also important to consider the total solar power absorbed by the secondary mirror when the antenna is pointed at the sun, which is

$$P_s = (1 - R_s) \cdot R_{eff} \cdot \frac{\pi D_p^2}{4} I_0 , \qquad (6)$$

or $P_s = 80$ W, which is significant but not likely to cause damage. A further consideration relative to the secondary mirror is direct illumination of the area behind the secondary, which includes the weather seal and chopper components. Normally, with the antenna focused at infinity, these would be shaded by the secondary, but they could be exposed if the secondary mirror is run as far towards the primary as possible with the antenna pointed at the sun. For a surface oriented perpendicular to the reflected solar radiation from the primary, the received intensity at the secondary would be approximately

$$I_s = R_{eff} \cdot \left(\frac{D_p}{D_s} \right)^2 \cdot I_0 , \qquad (7)$$

or 8.2 kW·m^{-2}, about 6 times I_0, which is a safe level for occasional exposure.

4. Sun off boresight axis

The most significant potential hazards to the antenna occur when the sun is off the boresight axis, by an angle large enough that the prime focus is no longer blocked by the secondary. For a given off-boresight position of the sun, the solar intensity on a particular part of the antenna can be calculated by direct numerical integration, described below. These calculations have been checked using the illumination analysis function in the ray tracing program ZEMAX-EE. However, ZEMAX-EE does not provide a means of calibrating the intensity scale, so it is mainly useful as a check on the spatial dependence of the calculated results.

With reference to Fig. 1, the antenna is described in a Cartesian coordinate system with the origin at the vertex of the primary, positive z axis along the boresight axis, and x and y axes in the two quadrupod planes. The surface of the primary may be defined parametrically in terms of (x, y) as

$$\mathbf{r_p} = \begin{pmatrix} x \\ y \\ \left(x^2 + y^2\right) / 4 f_p \end{pmatrix} . \qquad (8)$$

The differential surface area of the primary is $J_p \cdot dxdy$, where J_p is the fundamental vector product

$$\mathbf{J_p} = \begin{pmatrix} x/2f_p \\ y/2f_p \\ 1 \end{pmatrix}, \tag{9}$$

and the local normal to the primary surface is

$$\mathbf{n_p} = \frac{\mathbf{J_p}}{|\mathbf{J_p}|}. \tag{10}$$

The vector from a general point $\mathbf{p}$ to the point on the primary surface corresponding to (x, y) is

$$\mathbf{r_i} = \mathbf{p} - \mathbf{r_p}, \tag{11}$$

and its reflection in the surface is

$$\mathbf{r_r} = \mathbf{n_p} \cdot (\mathbf{r_i} \cdot \mathbf{n_p}) - \mathbf{n_p} \times (\mathbf{r_i} \times \mathbf{n_p}). \tag{12}$$

If $\mathbf{r_r}$ is directed towards the sun, then the contribution dI to the intensity at $\mathbf{p}$ received by a surface with unit normal $\mathbf{n}$, from a projected element of area $dxdy$ at $\mathbf{r_p}$ is

$$dI = R_{eff} B_{sun} \frac{(\mathbf{J_p} \cdot \mathbf{r_i}) \cdot (-\mathbf{r_i} \cdot \mathbf{n})}{|\mathbf{r_i}|^4} dxdy, \tag{13}$$

where $B_{sun} = 2.1 \cdot 10^7$ W·m^{-2}·sr^{-1} is the apparent brightness of the sun. Finally, the total intensity incident upon a surface at $\mathbf{p}$ with unit normal $\mathbf{n}$ directed towards the primary reflector is then

$$I = \iint \Phi(\mathbf{r_r}, \mathbf{u_{sun}}) \cdot \Theta(\mathbf{r_i}, \mathbf{n}) \cdot dI, \tag{14}$$

where the range of integration is over the projected disk of the primary, $\mathbf{u_{sun}}$ is a unit vector directed towards the center of the sun's disk,

$$\Phi(\mathbf{r_r}, \mathbf{u_{sun}}) = \begin{cases} 1 \text{ if } \dfrac{|\mathbf{r_r} \times \mathbf{u_{sun}}|}{|\mathbf{r_r}|} < \sin(\alpha_{sun}/2) \\ 0 \text{ otherwise} \end{cases} \tag{15}$$

is a function which keeps track of whether $\mathbf{r_r}$ points within the sun's disk, and

$$\Theta(\mathbf{r_i},\mathbf{n}) = \begin{cases} 1 & \text{if} \quad \mathbf{r_i}\cdot\mathbf{n} < 0 \\ 0 & \text{otherwise} \end{cases} \tag{16}$$

is a function which rejects rays approaching the surface from behind.

The worst-case solar intensity incident on any part of the antenna occurs when the sun is a few degrees off the boresight axis, in one of the two planes defined by the quadrupod. This case is illustrated schematically in Fig. 2. As the sun moves off boresight, a distorted image of the sun grazes the bottom edge of the aluminum quadrupod cover. The bottom of the cover has the V-profile shown in Fig. 2, mainly to enhance the RF performance of the antenna, but with the added benefit of spreading the incident solar radiation over a larger area. The intensities calculated by integration of Eq. (14), for points along the bottom of the quadrupod cover, are plotted in Fig. 3 for the sun at 6°, 9°, and 12° off boresight, in the x-z plane of Fig. 2. For each boresight angle, the plotted curves give the intensity as a function of the distance x from the antenna axis, for three y-offsets corresponding to the bottom ridge of the quadrupod cover (y = 0 mm), just off the ridge (y = 5 mm), and the outer edge of the cover (y = 28 mm). Blockage of the reflected sunlight by the subreflector assembly has been ignored, so the values presented are an overestimate by as much as 20% for the sun 6° off boresight.

The worst case occurs with the sun 6° off boresight, for which the peak intensity incident on the ridge of the cover is 200 kW/m^2 (20 W/cm^2). This is high enough to cause local heating which could be expected to damage cables that come into contact with the inside of the cover. This problem can be avoided by dressing the subreflector cabling well away from the bottom edge of the cover, and out of contact with the sides of the cover.

Under sustained exposure to the sun's image, as might occur when tracking a source close to the sun, the entire quadrupod cover will heat up. The average temperature of the cover will initially rise at the rate

$$\frac{dT}{dt} = \frac{P}{\rho ChA} \tag{17}$$

where $\rho = 2.7$ g·cm^{-3} and $C = 0.9$ joule·g^{-1}·K^{-1} are the density and heat capacity of aluminum, respectively, $h = 1.6$ mm is the cover thickness, and $A = 0.4$ m^2 is the area of the upper cover. The total power P absorbed by the cover may be estimated, in the worst case, by assuming that the entire image of the sun falls on the cover. Then P may be obtained from Eq. (6), taking $R_s = 0.5$ as an estimate for the reflectivity of the clear anodized finish of the cover. Then $P = 400$ W, and $dT/dt = 0.25$ K·s^{-1}. Consequently, slewing the antenna rapidly past the sun will not cause the overall cover temperature to rise significantly. If, on the other hand, the antenna is tracking a source near the sun, such that the sun's image dwells on the quadrupod cover for at least several minutes, then the steady-state average temperature rise ΔT of the cover, neglecting conduction to the lower cover and quadrupod leg, will be approximately

$$\Delta T = P \cdot \frac{MR}{A} \tag{18}$$

where MR, the thermal resistance of the cover-air boundary layer, ranges from $MR \approx 0.04$ m^2·K·W in a light wind (~3.5 m·s^{-1}) to $MR \approx 0.12$ m^2·K·W in still air [ASHRE

Handbook of Fundamentals (1977)]. The corresponding range of ΔT is $\Delta T \approx 40$ K in light wind and $\Delta T \approx 120$ K in still air. The latter figure, though based on what are expected to be conservative assumptions, is nevertheless high enough that tests should be made to validate these estimates, before the antennas are permitted to track continuously near the sun. Such tests should employ at least two temperature sensors on the quadrupod cover, spaced at least 0.2 m apart, so that at least one sensor is away from the zone directly heated by the sun's image.

5. Solar observing

It is impossible to damage the receivers, or the cryostat windows, by pointing the antenna at the sun. Even if the Goretex window on the elevation axis is not in place, M4 intercepts less than 4% of the sun's image at the Cassegrain focus. Furthermore, any radiation traveling beyond M4 must reflect off at least one polarizing grid before arriving at the cryostat windows. For solar observing, the only provision which needs to be made for the receivers is to prevent receiver saturation, by inserting an attenuator in the beam path. Assuming a brightness temperature of approximately 6000 K for the sun, the required attenuation is of order 13 dB. The optimum calibration strategy would likely be to independently calibrate the attenuator loss spectrum in the laboratory, and insert the attenuator between the SMA calibration unit and the sky.

As mentioned above, when the antenna is pointed at the sun there is an additional heat load of some 80 W on the secondary mirror. This could increase over time as the surface of the mirror ages. Consequently, the temperature of the chopping secondary assembly should be monitored during solar observations.

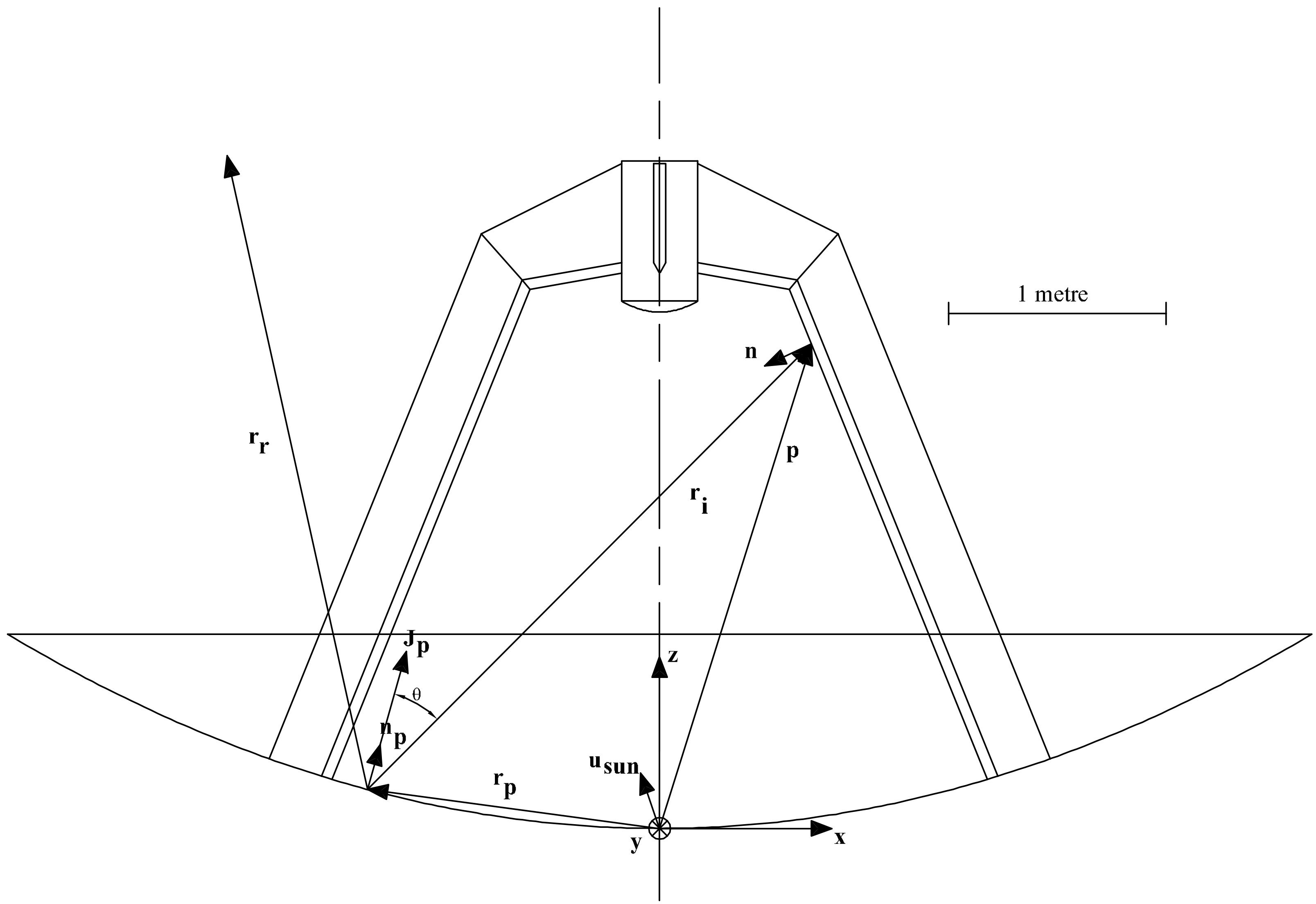
1 metre
r_r
n
p
r_i
J_p
θ
z
n_p
u_sun
r_p
y
x

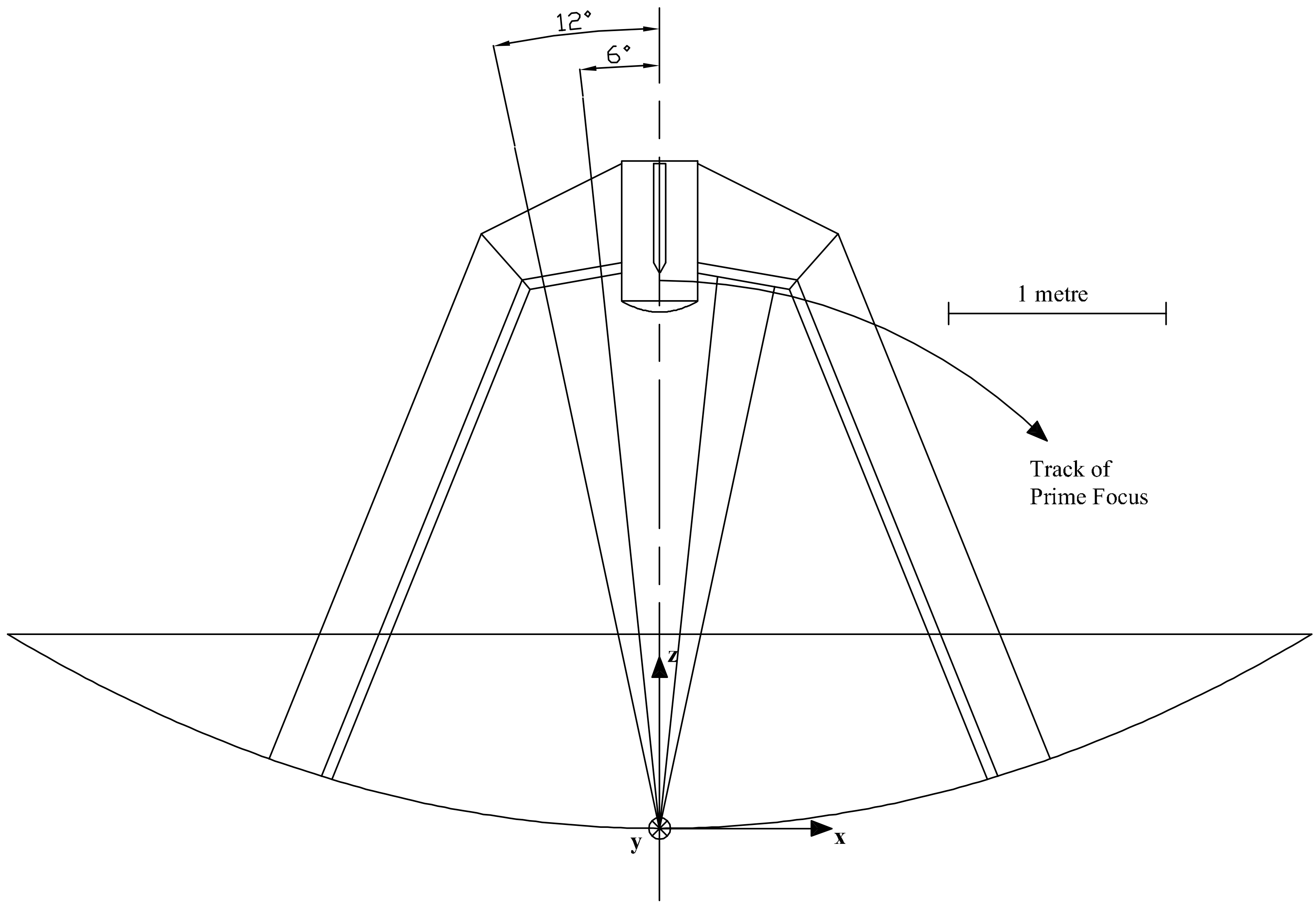
12°
6°
1 metre
Track of
Prime Focus
z
x
y

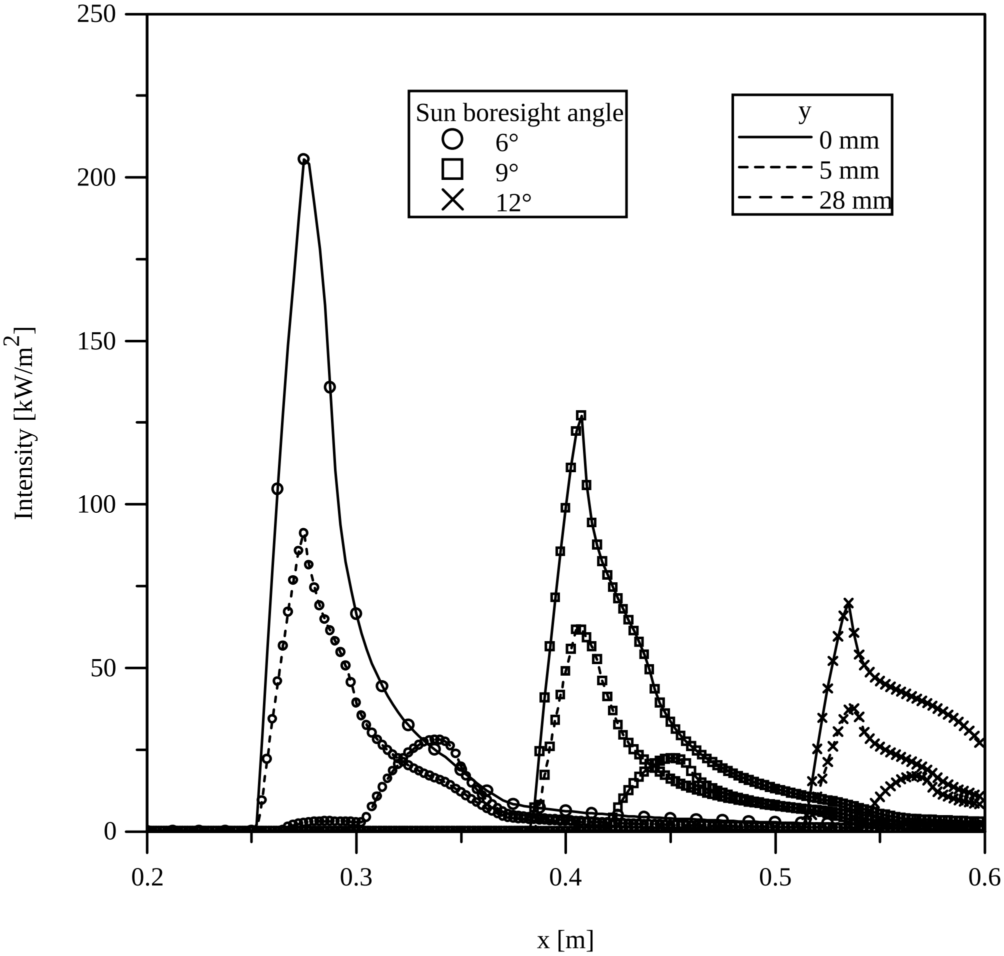

Sun boresight angle
6°
9°
12°
y
0 mm
5 mm
28 mm
Intensity [kW/m2]
x [m]
250
200
150
100
50
0
0.2
0.3
0.4
0.5
0.6